



SplitCore: An exceptionally versatile viral nanoparticle for native whole protein display regardless of 3D structure

Andreas Walker^{1,2*}, Claudia Skamel¹ & Michael Nassal¹

¹University Hospital Freiburg, Dept. of Internal Medicine II / Molecular Biology, D-79106 Freiburg, Germany, ²Faculty of Biology, University of Freiburg, D-79104 Freiburg, Germany.

SUBJECT AREAS:
NANOBIOTECHNOLOGY
PROTEIN DESIGN
STRUCTURAL BIOLOGY
VACCINES

Received
19 January 2011

Accepted
10 March 2011

Published
14 June 2011

Correspondence and
requests for materials
should be addressed to
M.N. (nassal2@ukl.
uni-freiburg.de)

* Current address:
Institute of Virology,
University of Duisburg-
Essen, D-45147 Essen,
Germany.

Nanoparticles displaying native proteins are attractive for many applications, including vaccinology. Virus-based nanoparticles are easily tailored by genetic means, commonly by inserting heterologous sequences into surface-exposed loops. The strategy works well with short peptides but is incompatible with the structures of most native proteins, except those with closely juxtaposed termini. Here we overcome this constraint by splitting the capsid protein of hepatitis B virus, one of the most advanced and most immunogenic display platforms, inside the insertion loop (SplitCore). The split parts, coreN and coreC, efficiently form capsid-like particles (CLPs) in *E. coli* and so do numerous fusions to coreN and/or coreC of differently structured proteins, including human disease related antigens of >300 amino acids in length. These CLPs induced high-titer antibodies, including neutralizing ones, in mice. The concept was easily expanded to triple-layer CLPs carrying reporter plus targeting domains, and should be applicable to protein-based nanoparticle design in general.

Viral capsids are natural self-assembling nanoparticles amenable to genetic modification, with diverse applications in material science^{1, 2} and biomedicine³ including vaccinology⁴. The icosahedral nucleocapsid of hepatitis B virus (HBV) is particularly well characterized in the latter aspect⁵. Authentic nucleocapsids are formed by 120 (triangulation number $T=4$; diameter ~ 34 nm) or to a lesser extent 90 dimers ($T=3$; diameter ~ 30 nm)⁶ of a single 183 amino acid (aa) core protein (HBc; reviewed in⁷); its N terminal ~ 140 aa are required for assembly^{8, 9}, the capsid-internal C terminal domain (CTD) binds nucleic acids. In the largely α -helical fold of the assembly domain^{10–12}, a hairpin formed by helices $\alpha 3$ and $\alpha 4$ serves as dimerization interface (Fig. 1a); the resulting four-helix bundles protrude from the capsid surface as prominent spikes. The exposed loop connecting $\alpha 3$ and $\alpha 4$ is part of the immunodominant c/e1 B-cell epitope between aa 74–84 which evokes >90% of the anti-HBc response during HBV infection¹³. HBc particles are exceptionally immunogenic, likely due to the repetitive surface presentation of B cell epitopes¹⁴, the presence of potent T cell epitopes, plus their ability to act as T cell independent antigen¹⁵. These properties contribute to the potent immunogenicity enhancement experienced by foreign sequences displayed on HBc CLPs, especially if inserted into the most surface-exposed, yet sequence-internal, c/e1 loop; however, such insertions must not compromise assembly competence.

Display of small peptides in the c/e1 loop is well established¹⁶, and HBc CLPs presenting a peptide from the circumsporozoite protein (CSP) of the malaria agent *Plasmodium falciparum* have proven safe in a Phase I study¹⁷; results with CLPs presenting an influenza A virus peptide are soon to be expected (ClinicalTrials.gov Identifier: NCT00819013). However, one or a few epitopes account neither for the genetic diversity and adaptability of pathogens nor for immunological polymorphisms in vaccinees; furthermore, peptides wedged into the carrier may adopt new, antigenically irrelevant structures¹⁸. Displaying native whole proteins would overcome these limitations¹⁹ and provide new opportunities also for non-vaccine applications. Successful whole-protein display has first been reported for terminal fusions to small bacteriophage λ and T4 accessory proteins that bind to preformed capsids^{20, 21}. However, due to their complexity these systems have not found wide-spread application. A much simpler access to protein-displaying particles was provided by our demonstration that HBc can present the 238 aa green fluorescent protein (GFP)²², as well as the outer surface protein C (OspC) of the Lyme disease agent *Borrelia burgdorferi* (Bb)²³, with those CLPs inducing neutralizing antibodies²⁴. Both proteins are exceptional in that their closely juxtaposed termini^{25, 26} fit naturally into the c/e1 acceptor sites. In contrast, proteins with farther apart termini interfere with assembly, as exemplified by Bb OspA²⁷. Bridging the distance with long connecting linkers was only partially effective, and although the mostly irregular multimers evoked protective

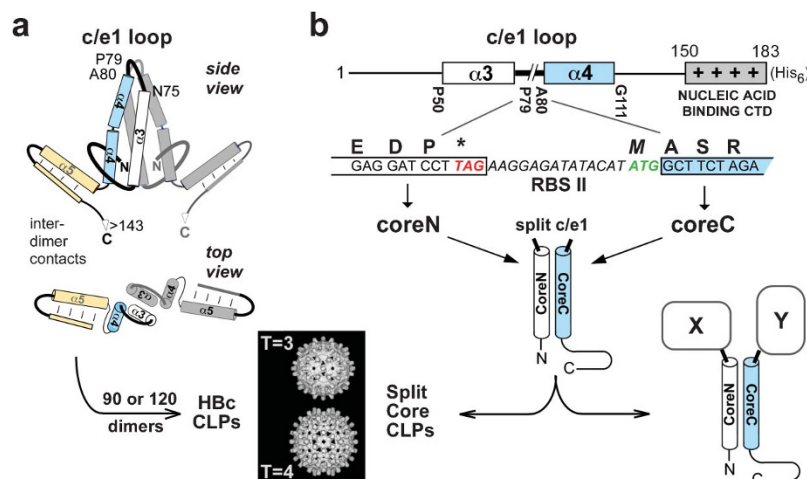


Figure 1 | Structural rationale of the SplitCore approach. (a) Scheme of the HBc assembly domain (aa 1–143), based on x-ray data (pdb:1QGT¹²). In the dimer (the second monomer is shown in grey), the $\alpha 3$ (white) - $\alpha 4$ (skyblue) hairpins associate into four-helix-bundles; the c/e1 epitope locates to the loop connecting $\alpha 3$ and $\alpha 4$. Helices $\alpha 1$ and $\alpha 2$ are omitted for clarity; $\alpha 5$ and the sequence to position 140 (orange) mediate multimerization of 90 or 120 dimers into T=3 and T=4 CLPs; cryo EM reconstructions are from ³⁴. The CTD (not shown) locates to the interior. (b) SplitCore concept. The HBC sequence was split inside c/e1 between P79 and A80 via artificial stop and start codons. Efficient co-expression in *E. coli* of coreN (aa 1–79) and coreC (aa 80–149 or 183) was achieved by bicistronic vectors with the 3' cistron controlled by a second ribosome binding site (RBS II), or via overlapping stop and start codons (e.g. Supplementary Fig. 2c). If the separate coreN and coreC fragments maintained the ability to assemble into HBc-like particles (left arrow), the resulting SplitCore CLPs would expose new termini on their surface, either of which could serve as one-sided, sterically unrestrained attachment site (right arrow) for heterologous molecules (X, Y).

antibodies ²⁸, structural heterogeneity and the unknown immunogenic potential of the linkers are undesirable for a vaccine.

Hence the conformational stress imposed on carrier and insert by the two-sided fixation emerged as key problem. Opening one of the two linkages should relieve this stress, as was corroborated by enhanced CLP formation by an HBc-OspA fusion upon site-directed cleavage via an engineered protease site ²⁹. However, the extra sequences and processing steps prompted us to seek a more general solution, leading to the “SplitCore” concept (Fig. 1b).

As in some non-multimerizing proteins ³⁰, fragment complementation of the separately expressed N and C terminal parts (coreN and coreC) of HBc split inside the c/e1 loop might yield CLP-forming split subunits. Foreign sequences fused to coreN and/or coreC would be attached to such CLPs via one end only and thus without imposing conformational stress, regardless of their structure (Fig. 1b, bottom right). The data reported below demonstrate the validity of this concept and suggest its applicability to protein-based nanoparticle scaffolds in general.

Results

Separately expressed coreN and coreC fragments assemble efficiently into HBc-like CLPs. Efficient complementation requires that the two fragments be expressed in near equimolar amounts, with minimal non-specific aggregation. This was best achieved by using bicistronic mRNAs (Fig. 1b). The original constructs encoded coreN (aa 1–79) and coreC (aa 80–149 or 80–183) in that order, each preceded by its own ribosome binding site (RBS). Alternative functional designs included overlapping stop and start codons (see Supplementary Fig. S2 online). For some fusion proteins (e.g. Supplementary Fig. S7 online), reversing the cistron order provided superior expression, likely due to differential start codon accessibility ³¹. Their functionality further excluded that read-through products comprising both fragments, as were occasionally formed (e.g. Supplementary Fig. S2), were required as association scaffolds.

Sucrose gradient sedimentation of cleared lysates from bacteria expressing coreN plus coreC149 (SplitCore149) or coreC183 (SplitCore183) revealed cosedimentation (Fig. 2a) of two peptides

of the expected sizes into the particle-typical center fractions ³², in yields of 10–15 mg/L of culture. Complementation was corroborated by native agarose gel electrophoresis (NAGE) where particles

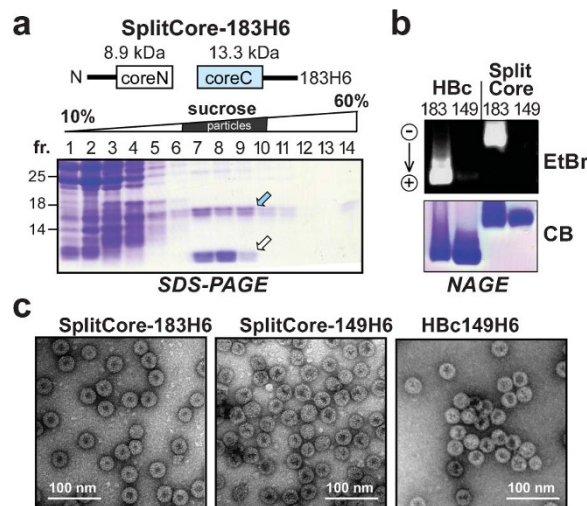


Figure 2 | Efficient assembly of split wild-type HBc. (a) Co-sedimentation in sucrose gradients of separately expressed coreN and coreC fragments (indicated by the downward pointing arrows) into particle-typical fractions. Cleared lysates from bacteria co-expressing coreN and coreC183H6 were sedimented through sucrose gradients, and aliquots of each fraction were analyzed by SDS-PAGE and Coomassie-Blue (CB) staining; coreN plus coreC149H6 and constructs lacking the His-tag gave comparable results. The somewhat lower than expected mobility of the coreC183H6 fragment observed in these and all subsequent experiments likely results from the high arginine-content of the CTD. (b) Native agarose gel electrophoresis (NAGE). Aliquots from the center gradient fractions were subjected to NAGE; particle-borne RNA was visualized by ethidium bromide (EtBr), protein by CB. (c) Negative staining EM of SplitCore and conventional HBc149_H6 CLPs. Additional structural and antigenic properties of SplitCore are shown in Supplementary Figure S1 online.



migrate as distinct bands⁸. Like contiguous HBC, the split 183 and 149 derivatives each produced a single band upon Coomassie Blue staining; their slower mobility (Fig. 2b, bottom) likely relates to changes in surface charge mediated by the new exposed termini. HBC CLPs containing the CTD package bacterial RNA^{8, 33} which can be stained with ethidium bromide. The same was observed for SplitCore183, proving integrity of the CLPs (Fig. 2b, top). Abundant intact particles were also detected by negative staining EM (Fig. 2c). These data demonstrate efficient self-complementation of coreN and coreC with and without CTD into assembly-competent structures.

Splitting HBC in *c/e1* preserves the global particle structure but destroys the immunodominant epitope and subtly affects others.

By high-percentage NAGE and direct evaluation of electron micrographs we observed an increased fraction of about 30–40% vs. ~5% T=3 particles for the SplitCore CLPs (see Supplementary Fig. S1). As insertions into *c/e1* can exert a similar effect³⁴, these data confirm independently that there is structural cross-talk between the spike tip and the C proximal multimerization sites³⁴. Immunoblotting of NAGE gels (see Supplementary Fig. S1 online) with monoclonal antibodies (mAb's) revealed a complete loss of *c/e1* reactivity whereas reactivity with the particle-specific mAb's 275¹³ and 3120³⁵ was only slightly reduced. Hence SplitCore CLPs mimic the structure of HBC though with subtle alterations in regions away from the spike tip. The absence of *c/e1* reactivity was also reflected in a 15- to 80-fold reduced reactivity of SplitCore and SplitCore-GFP CLPs (see below) with anti-HBC antibodies from human serum in three widely used diagnostic anti-HBC assays (see Supplementary Fig. S1 and Supplementary Protocols online).

SplitCore-CLPs can natively display GFP fused to either coreN or coreC. Next we tested whether the SplitCore system is compatible with native surface display of a heterologous protein. GFP is an ideal model²² because chromophore formation depends on native folding. Constructs with GFP fused to either coreN or coreC were well expressed, including from a stop/start vector (see Supplementary Fig. S2 online), cosedimented in sucrose gradients, and ran as

distinct, green fluorescent bands in NAGE (see Supplementary Fig. S2); similar results were obtained with the coreC149 constructs and with GFP replaced by the red fluorescent mCherry (T.T.A. Nguyen and M. Nassal, unpublished results). Also Bb OspC fused to coreN formed CLPs with comparable efficiency (see Supplementary Fig. S3 online) as the previously described contiguous chain construct²⁴; hence for such favorable structures the SplitCore platform is as suited as conventional HBC.

SplitCore allows CLP presentation of an unfavorably structured protein that prevents CLP formation in the conventional HBC system.

The extended structure of OspA (Fig. 3, and Supplementary Fig. S4) is incompatible with efficient CLP formation upon *c/e1* insertion²⁸ (Fig. 3a, coreOspA183H6). In contrast, OspA fused to either coreN or coreC, and thereby exposing different parts of OspA (see below), efficiently formed regular CLPs, as indicated by sedimentation (see Supplementary Fig. S4 online) and EM (Fig. 2a, coreN-OspA183H6, OspA-coreC183H6). Similar results were obtained with coreC149 constructs (data not shown).

For immunogenicity evaluation, the further purified (see Supplementary Fig. S4 online) and endotoxin-depleted³⁶ CLP preparations were used to immunize mice as described²⁸ and Supplementary Information, lipidated (Pam3-Cys) OspA (LipOspA), the active ingredient of the commercial Lymex vaccine in which the lipid acts as TLR agonist, served as reference. While details will be reported elsewhere (A. Walker, T. Stehle, R. Wallich, M. Simon and M. Nassal, manuscript in preparation) the most pertinent results were: (i) both CLP preparations, and OspA-coreC in particular, induced higher levels of OspA-specific antibodies than LipOspA (Fig. 3b); (ii) in an established mouse model of Lyme disease³⁷, passive transfer of the antisera to coreN-OspA and Lymex protected 6 of 6 and 5 of 6 animals, respectively, from chronic Bb infection whereas only 1 of 6 mice was protected by the OspA-coreC induced antibodies (Fig. 3c). This result is rationalized by the location of the major neutralizing epitope, LA2, in the C terminal part of OspA³⁸ which is solvent-exposed in coreN-OspA but not OspA-coreC CLPs (Fig. 3a); indeed, the

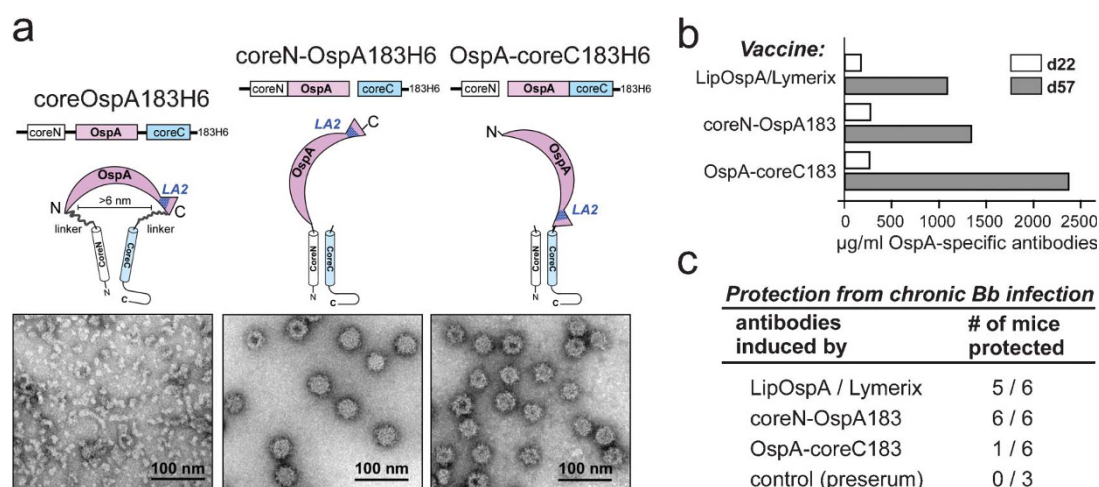


Figure 3 | Drastically enhanced CLP formation by SplitCore OspA fusions, and distinct immunological properties of SplitCore-OspA CLPs. (a) The ectodomain (aa 18–273) of Bb OspA adopts an extended β -sheet structure, with N and C terminus >6 nm apart (see Supplementary Fig. S4a for more details). Conventional insertion into *c/e1* required very long linkers to generate soluble, though rarely regular particle forming, aggregates (left). In contrast, SplitCore with OspA fused to either coreN or coreC efficiently formed regular CLPs. Depending on orientation, the neutralizing LA2 epitope³⁸ is solvent-exposed, or buried. (b) SplitCore-OspA CLPs induce comparable if not higher anti-OspA antibody titers than the LipOspA Lymexix vaccine. Groups of 5 Balb/c mice each were immunized with 10 μ g each of the indicated CLPs (endotoxin content <50 EU/mg protein) or LipOspA on day 0, 14, 18 and 49. anti-OspA titers (in μ g/ml serum) in sera collected at day 22 and 57 are shown. (c) Protectivity against chronic Bb infection. The indicated immune sera were transferred into SCID mice, and the animals were challenged with 10^4 borreliae (strain ZS7) each. Development of arthritic disease was monitored over 52 days²⁸; animals remaining symptom-free were considered protected from chronic infection. The low protective potential despite high overall anti-OspA titer of the OspA-coreC183 induced immune sera correlated with a 4- to 5-times lower content in LA2-equivalent antibodies (A. Walker, T. Stehle, R. Wallich, M. M. Simon, and M. Nassal; manuscript in preparation).



fraction of LA2-equivalent antibodies was drastically lower (not shown). Thus the SplitCore system allows to deliberately direct antibodies against a specific antigen region, with potentially relevant consequences for protectivity.

SplitCore-CLPs can display near full-length *P. falciparum* CSP and induce very high titer anti-CSP yet lower titer anti-HBc antibodies. Next we tested the SplitCore system's ability to display an even larger protein, CSP, from *Plasmodium falciparum*. CSP consists of ~400 aa (Fig. 4a), including an immunodominant central repeat region with a variable number (~40) of repetitions of NANP and fewer NVDP motifs³⁹. Two of the most advanced, yet only modestly protective, malaria vaccine formulations are RTS,S³⁹ and ICC-1132¹⁷. RTS,S comprises the C terminal half of CSP without the GPI anchor signal fused to the small HBV surface protein (HBs); ICC-1132 features several of the central repeat motifs inserted into HBc c/e1 plus the CSP universal T cell epitope fused to the HBc149 C terminus. Beyond the much lower intrinsic immunogenicity of HBs vs. HBc antigen⁴⁰, the lack in either vaccine of potentially important epitopes in the N terminal CSP sequence⁴¹ may limit their efficacy. Here we fused the 319 aa CSP sequence from the well characterized derivative CS27IVC⁴² to coreN. A conventional c/e1 insertion construct was completely insoluble, but the SplitCore versions (with coreC149H6 and coreC183H6) efficiently formed CLPs (see Supplementary Fig. S5 online); EM revealed abundant particles with a regular inner and a more elaborate, often ninja-star-like outer shell (Fig. 4c), consistent with the recently proposed extended rod-like structure of CSP⁴¹.

For immunogenicity testing further purified SplitCoreN-CSP149 CLPs (see Supplementary Fig. S5 online) were used to immunize mice⁴³ and Supplementary Information; a conventional repeat peptide construct (HBc149-NANP) analogous to ICC-1132 (Fig. 4b) served as reference (A. Walker, J. Billaud, D. Milich, M. Nassal; manuscript in preparation). Either CLP induced very high titers of NANP peptide-specific antibodies. When tested against recombinant CSP, the antisera induced by the CSP-presenting CLPs gave even stronger signals, likely owing to the presence of additional antibodies recognizing

non-NANP epitopes; in contrast, anti-HBc titers were 5- to 20-fold lower. Hence SplitCore-CSP CLPs may overcome shortcomings of both RTS,S and ICC-1132, warranting further investigation of their protective potential.

Triple-layer fluorescent SplitCore CLPs exposing a targeting domain. Next we evaluated the ability of SplitCore CLPs to simultaneously present two different sequences per split subunit. As a model for a heterodimeric insert, we chose split GFP because of its known self-complementation ability when separated at various sites³⁰. Furthermore, the GFP-internal new termini, if exposed, might allow to add yet another protein shell around the HBc scaffold (Fig. 5a); finally, GFP provides a convenient reporter to monitor how such additional domains affect the properties of the CLPs. A solubility-enhanced GFP variant was split in the loop between β -strands 10 and 11 of the barrel structure⁴⁴ so as to expose the splitting site to the solvent; GFP β 1-10 was fused to coreN, and GFP β 11 to coreC. The resulting SplitCore-SplitGFP (SC-SGFP) protein was well expressed in largely soluble, particulate and fluorescent form (see Supplementary Fig. 6 online).

As a third domain, we fused the B1 immunoglobulin-binding domain from protein G (GB1) to the GFP β 11-coreC fragment (Fig. 5). GB1 is relatively small (56 aa) but retains a high affinity for immunoglobulins. The bipartite triple fusion termed SC-SGFP-GB1 was highly expressed (~40 mg soluble protein/L culture), and efficiently formed fluorescent CLPs according to sedimentation, NAGE analysis and EM (Fig. 5b-d). Immunoglobulin binding was demonstrated by indirect immunofluorescence microscopy (Fig. 5e), where the CLPs generated a very similar, primary antibody-dependent staining pattern as an Alexa-488 conjugated secondary antibody. SC-SGFP-GB1 CLPs could also substitute for dye-labeled secondary antibody in fluorescent Western blots with comparable sensitivity (Fig. 5f), and they detected antibody-decorated cells in flow cytometry (A. Walker, PhD thesis, University of Freiburg, 2008).

The small GB1 domain does not push the system to its limits. We have successfully generated fluorescent SplitCore CLPs with OspC fused to coreN-GFP β 1-10, or to GFP β 11-coreC; and with OspA

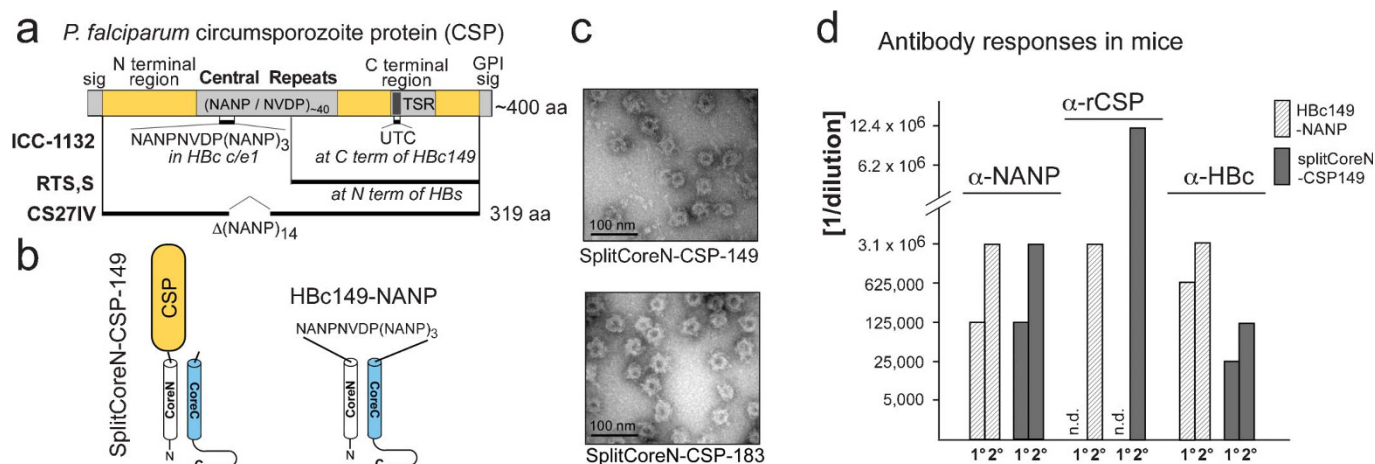


Figure 4 | SplitCore-CLPs can display the entire *P. falciparum* circumsporozoite protein (CSP) ectodomain. (a) General organization of CSP. CSPs are ~400 aa in length, with an N terminal signal sequence and a C terminal glycosylphosphatidylinositol (GPI) anchor signal. The central region contains a variable number of NANP and fewer NVDP repeats (~40 total), the C proximal region a thrombospondin type-1 repeat (TSR) including a universal T cell epitope (UTC). Experimental vaccine ICC-1132 carries a few of the repeats inserted into c/e1 of HBc, plus the UTC fused to the C terminus¹⁷; vaccine RTS,S comprises the C terminal half of CSP except the GPI signal, fused to the small surface antigen (HBs) of HBV³⁹. CS27IVC⁴², based on the T4 isolate/Thailand (Genbank accession no. M19752), lacks the terminal signals and 14 NANP repeats. (b) Schematic structures of SplitCoreN-CSP-149, carrying the entire CS27IVC sequence, and Hbc149-NANP. (c) CLP formation by SplitCoreN-CSP-149 and -183 revealed by negative staining EM. (d) Antibody responses in mice against (NANP)₅ peptide (α -NANP), recombinant CS27IVC protein (α -rCSP), and HBc. (B10.xB10.S) F1 mice were vaccinated with 20 μ g each of low endotoxin (<40 EU/mg protein) preparations of SplitCoreN-CSP149 (Supplementary Fig. S5) or Hbc149-NANP CLPs in incomplete Freund's adjuvant (IFA) and boosted once 56 days later with 10 μ g antigen in IFA. Antibody responses after the first (1^o) and second immunization (2^o) were assessed by ELISA via antiserum dilution series⁴³; the highest dilution giving a signal at least three-fold above background (pre-immune sera) is indicated.

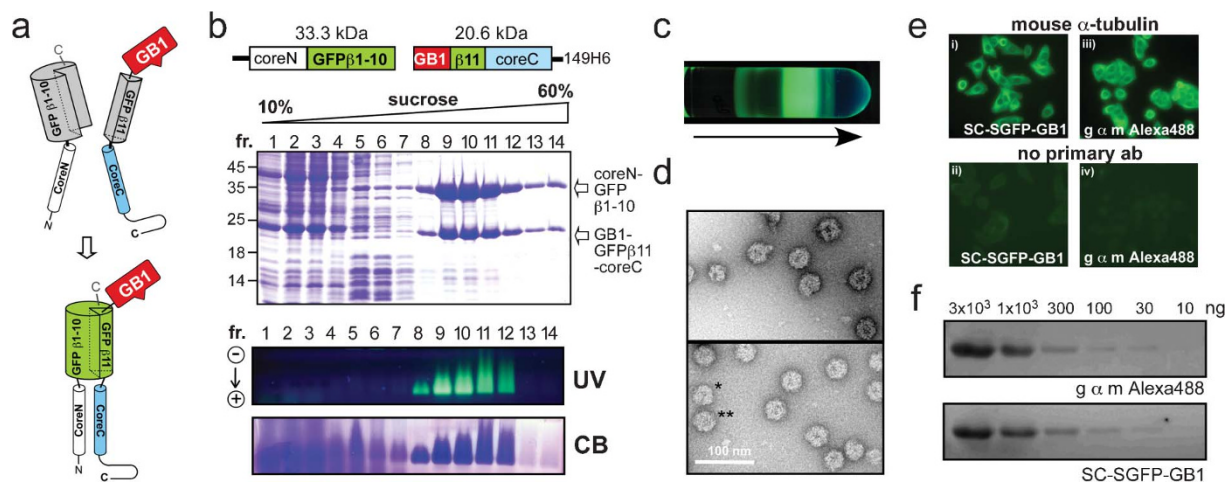


Figure 5 | SplitCore-SplitGFP-GB1: Triple-layer fluorescent particles with exposed targeting domains. (a) Design of SplitCore-splitGFP-GB1 fusions (SCSGFP-GB1). GB1 fused to one of the new ends provided by the split GFP insert (see Supplementary Fig. S3 online) should yield fluorescent CLPs with exposed immunoglobulin binding GB1 domains. (b) Expression and CLP formation. Bacterial lysates were subjected to sedimentation as in Fig. 1c. SDS-PAGE (top) demonstrated cosedimentation of two proteins of the expected sizes into fractions 8 to 12 which produced distinct green fluorescent bands in NAGE (UV) that also stained with CB. Similar results were obtained with GB1 fused to GFPβ1-10 on coreN (not shown). (c) Visualization of folded GFP containing material in the gradient tube from which the samples in (b) were derived. (d) Negative staining EM. The two micrographs are from independent grids onto which material from fraction 8, diluted 10-fold in PBS, was applied. Smaller (*; diameter ~38 nm) and larger (**; diameter ~42 nm) particles were observed. (e,f) SCSGFP-GB1 binds antibodies. (e) Indirect immunofluorescence. Permeabilized HeLa cells were incubated with mouse anti-tubulin antibody (i, iii) or not (ii, iv), then with SCSGFP-GB1 (i, ii) or an Alexa488-conjugated goat anti-mouse IgG (gαm-Alexa488) antibody (iii, iv). Both generated similar, primary antibody-dependent staining patterns. (f) Fluorescent Western blot. Decreasing amounts of GFP were separated by SDS-PAGE, blotted on nitrocellulose and incubated with a mouse anti-GFP mAb mixture (Roche), then with either gαm-Alexa488 or SC-SGFP-GB1. Fluorescent signals were detected using a Typhoon 7000 imager (GE Healthcare).

fused to the N terminus of GFPβ11-coreC and even to both core fragments (see Supplementary Fig. S7 online). That construct encompasses a total mass of ~100 kDa of heterologous sequence per 15 kDa carrier subunit. We also obtained CLPs by fusing an attenuated variant of *S. aureus* enterotoxin B (SEB⁴⁵) to GFPβ11-coreC (Supplementary Fig. S7). SEB comprises ~240 aa, and in the contiguous HBC system had not produced any soluble fusion protein (J. Vorreiter, B. Stiles, M. Nassal; unpublished data).

SplitCore is adaptable to the core proteins of other hepadnaviruses. Preexisting immunity to a carrier might limit repeated applications via “carrier induced epitopic suppression”⁴⁶ although for some HBC-presented antigens there is even evidence for the opposite^{47, 48}. Perhaps more important for human vaccines, tolerance against HBC in chronic HBV carriers could limit immune enhancement by carrier dependent T cell responses. This may be circumvented by using core proteins from rodent (woodchuck, ground squirrel) hepadnaviruses⁴³ which diverge by ~40% in their sequences from HBC (see Supplementary Fig. S8a online).

Split woodchuck core protein (SplitWHc) efficiently formed CLPs, as based on sedimentation, NAGE and EM (see Supplementary Fig. S8 online), and was able to display full-length OspA and CSP (not shown). Immunogenicity in mice of the SplitWHc CSP-CLPs was comparable to that of the respective HBC CLPs (A. Walker, J. Billaud, M. Nassal, D. Milich; manuscript in preparation), with generation of very high levels of NANP-specific and relatively low levels of anti-carrier antibodies (see Supplementary Fig. 8 online). Furthermore, CLPs formed when coreN was derived from one and coreC from the other virus (A. Walker, PhD thesis, University of Freiburg, 2008), consistent with a substantial sequence tolerance of coreN - coreC association.

Discussion

Genetic insertion of heterologous sequences into surface-exposed loops of viral capsid proteins provides convenient access to tailored

nanoparticles⁴. However, insertion of native proteins nearly always suffers from structural incompatibility. The SplitCore approach overcomes this fundamental restriction for HBC, one of the most attractive carrier scaffolds to date⁵, and provides access to particles with sophisticated surface structures as illustrated in Fig. 6a. The same concept should be applicable to other protein-based nanoparticles including for, but not limited to, vaccine applications.

To our knowledge, SplitCore is the first truly multimeric split protein (for a compilation of previously established split protein systems, see reference⁴⁹). Efficient association of the coreN and coreC fragments may be promoted by the extensive contacts provided by the α3 - α4 hairpin interface (Fig. 1); this should allow for flexibility regarding choice of the exact splitting site. The insolubility of either fragment expressed alone (not shown) suggests that the bicistronic mRNA design also promotes fragment association by providing spatial proximity during translation. Efficient CLP formation with various differently structured heterologous proteins (Figs. 3–5; Supplementary Figs. S2–S7) indicates that many more will be displayable on SplitCore CLPs, regardless of tertiary structure. Though some restrictions remain, including very large size (exceeding the geometrically restricted space available on the CLP surface), quaternary structure (e.g. antiparallel dimers, higher order multimers; see³²), or inability of the heterologous protein as such to be solubly expressed in *E. coli* (e.g. membrane proteins, glycoproteins), a multitude of protein antigens remain for vaccine applications. Particularly useful is the SplitCore-intrinsic ability to generate opposite surface orientations, allowing to control specificity of the anti-insert immune response (Fig. 3). If neutralization is not as confined to a specific spatial location as in OspA, mixing CLPs presenting the antigen in either orientation provides an easy route to broaden the anti-insert antibody repertoire.

A point to consider for using HBC as vaccine carrier in humans is that anti-HBC testing is used diagnostically to distinguish HBV infection (routinely resulting in a long-lasting anti-HBC response) from anti-HBV vaccination (with HBs, and thus without inducing



anti-HBc). Our data show that disruption of the immunodominant *c/e1* epitope and, on top, sterical shielding by the displayed whole proteins strongly reduce the anti-HBc response (Fig. 4d and Supplementary Fig. S8 online); this was also reflected by the much reduced reactivity of SplitCore CLPs with patient serum anti-HBc (Supplementary Fig. S1 online). Furthermore, SplitCore CLP-induced vs. infection-induced anti-HBc antibodies are easily distinguished by the absence of any anti-*c/e1* response. If considered necessary, animal HBV based SplitCore CLPs may be used instead (Supplementary Fig. S8 online). Finally, cross-complementation between HBc- and WHc-derived coreN and coreC implies that undesired epitopes may be eliminated via engineered mutations.

Because of its exceptional immunological properties, most previous efforts towards manipulating HBc were devoted to its use as a vaccine carrier. However, the SplitCore system also opens new avenues to nanoparticle design in general. The surface-exposed termini of SplitCore-displayed heterologous proteins, either on a genuinely extended structure (X_u in Fig. 6b), or on a split insert (split X_f in Fig. 6b), can be used to build sophisticated multilayer architectures. Just one example are the SC-SGFP-GB1 CLPs, in which the HBc parts provide the particle scaffold, GFP an easily followable reporter, and GB1 a specific targeting device. Successful CLP formation with different proteins much larger than GB1 (Supplementary Fig. S7) indicates few limitations for the targeting domain. Moreover, the inner CLP lumen can serve as a cargo container. One example is CTD mediated packaging of RNA⁸ which, in vaccine applications, can act as a TLR7 agonist⁵⁰; hence coreC149 vs. coreC183 derivatives may be exploited to modulate the type of immune response induced. The CTD can be replaced by heterologous sequences (Z in Fig. 5) of up to ~17 kDa⁵¹, which might themselves have specific functionalities, including binding of non-nucleic acid and non-peptidic ligands that could serve as cargo. With appropriate targeting structures on their surface, such internally modified CLPs could be envisaged as specific delivery vehicles.

The SplitCore-intrinsic surface exposure of two accessible new termini also provides distinct advantages for enzymatic and chemical modification. An example is the display of a biotin-acceptor peptide

which can be biotinylated by the *E. coli* BirA ligase; such CLPs do indeed specifically interact with streptavidin (see Supplementary Fig. S9). Many other enzymatic modifications require accessible termini, amongst them sortase-mediated tagging⁵² and N terminal fatty acylation. According to our preliminary data (T.T.A. Nguyen and MN) myristoylation via N-myristoyl-transferases can efficiently be achieved when a suitable substrate sequence is exposed on the SplitCore CLPs. Chemical conjugation has greatly been advanced by bioorthogonal “Click” chemistries⁵³. Site-specific incorporation of Click-compatible non-natural amino acids into conventional HBc has been reported but the Click adducts were incompatible with CLP integrity⁵⁴, most likely because of sterical strain. Evidently, this would be overcome by adding the non-natural amino acids to coreN or coreC.

Various other viral capsid proteins are explored as display scaffolds⁴ yet up to now the ~400 aa Flock House virus coat protein is the only one for which native surface display of a complete protein, the anthrax receptor 2 (ANTRX2), has been achieved by genetic insertion⁵⁵; that protein was chosen because, as in GFP, its termini fit naturally into surface-exposed loops. Given that the sterical constraints for loop insertions are fundamentally similar in any protein, the advantages of the split capsid protein concept demonstrated here for HBc should as well be applicable to numerous other protein-based nanoparticle carriers.

Methods

Plasmid constructs. Parental plasmids pET28a2-HBc183H6 and pET28a2-HBc149H6³² feature a T7 promoter controlled synthetic HBc gene⁵⁶ encoding full-length (183) or truncated (149) HBV core protein (HBV genotype D, serotype ayw; accession no.: CAA 24706) with a C terminal His₆ tag. SplitCore derivatives were generated by introducing between HBc codons P79 and A80 a stop codon, a second RBS, and an initiator codon (Fig. 1b); in stop-start vectors the stop codon of coreN overlapped with the start codon of coreC (Supplementary Fig. S2c); in some cases, the cistron order was reversed (Supplementary Fig. S7e). All constructs were generated using standard PCR methods and verified by DNA sequencing.

Insert protein coding sequences. Plasmids used as sources for the genes of GFP²², OspA²⁸ and OspC_a²⁴ have previously been described. For CSP, plasmid pDS56-32/RBSII-CS27iVC_6XHis⁴² was obtained from the Malaria Research and Reference Reagent resource (MR4; code MRA-272). A plasmid encoding genetically attenuated

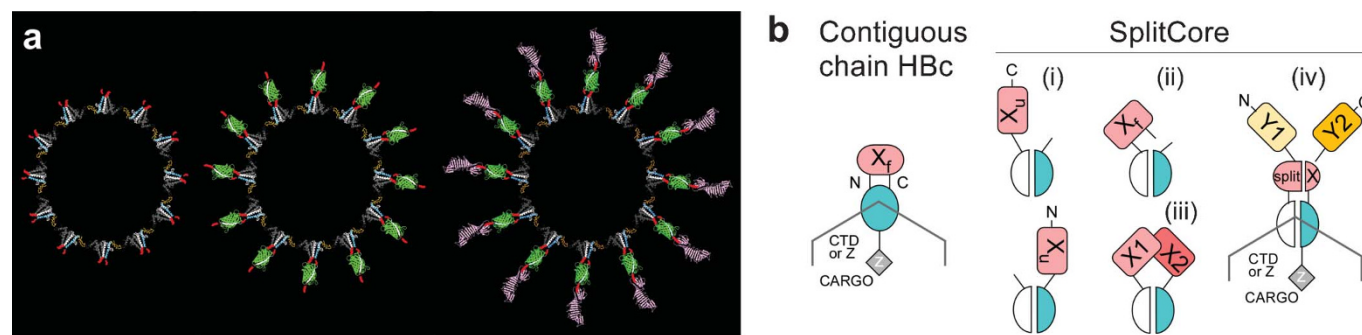


Figure 6 | Summary of unique SplitCore features. (a) Graphical illustration of representative, increasingly complex SplitCore CLPs generated in this study. The structural models of each protein are drawn approximately to scale; heterologous molecules fused to the second subunit per HBc dimer (grey) have been omitted for clarity. The cross-sections shown are hypothetical and only serve to illustrative pertinent SplitCore features. Splitting the insertion loop in HBc (left) leaves two surface-accessible termini (in red) for fusion of heterologous proteins regardless of their 3D structure. A protein with a favorable structure for insertion, such as GFP (middle), may itself be split to provide new exposed termini, to which an additional protein, such as OspA (right), can be added. The accessible termini on SplitCore, or the second or third layer proteins, are as well available for other types of modification. (b) Schematic comparison of the conventional contiguous chain HBc vs. SplitCore platforms. The half-hexagon symbolizes the icosahedral particle shell. In conventional HBc (left) surface presentation by *c/e1* insertion of foreign protein ligands X is restricted to the few having a naturally favorable structure (X_f). The CLP lumen may be modulated by C terminal modifications; the authentic CTD packages RNA as cargo but may be replaced, within limits (<17 kDa⁵¹), by heterologous moieties (Z) that could act as cargo or provide specific functions (ligand binding, reporter probes). In SplitCore the new exposed termini allow (i) presentation of unfavorably structured inserts (X_u) in either orientation; of X_f ligands with comparable efficiency as in the contiguous system (ii); and of two ligands per carrier subunit (iii). Solvent-exposed termini of X_u ligands may directly be used as further attachment sites (not tested); however, as demonstrated, this is definitely possible for a split X_f ligand like GFP. Particle-internal features can be manipulated as in contiguous chain HBc. One out of various applications are CLPs carrying a targeting ligand (Y1, Y2), a monitoring reporter (split X), plus a cargo specified by Z.



S. aureus enterotoxin B (SEB; mutations: L45F, Y89A, Y94A⁴⁵) was kindly provided by Dr. B. Stiles.

Junction sequences in individual constructs. The linkers connecting coreN or coreC with the inserts were typically G₄S or G₄T. In the SplitCore OspA fusions the original linkers ((G₄S)₂; (G₄S)₂RG₄DLLG₄) from the contiguous construct²⁸ were maintained for comparability. SplitGFP was based on a solubility enhanced version⁴⁴; the N terminal part consisted of GFP aa 1–214 (GFPβ1–10), followed by the dipeptide DP; GFPβ11 contained the sequence 214–238, preceded by an artificial initiator codon.

Protein Expression and Purification. *E. coli* BL21(DE3) Codonplus cells (Stratagene) were used throughout as described^{24,29,32}. Conditions for sedimentation through 10–60% sucrose step gradients at 20°C were as follows, depending on sample volume: SW28 rotor, 3:45 h at 28,000 rpm²⁴; TST41.14 rotor 2 h at 41,000 rpm; TLS-55 rotor, 45 min at 55,000 rpm. Gradients were harvested in 14 fractions (2.6 ml each for SW28; 860 µl each for TST41.14; 100µl each for TLS-55) from the top. For further purification, the pooled center gradient fractions were dialysed against TN150 buffer (25 mM Tris-Cl [pH7.5], 150 mM NaCl) and subjected to a second gradient sedimentation or size exclusion chromatography on Superose 6 (GE Healthcare).

Endotoxin depletion. Endotoxin was depleted by phase separation with Triton X-114 essentially as described³⁶. Residual detergent was depleted by repeated dialysis against excess PBS at 4°C. Endotoxin contents dropped from 10²–10⁶ EU/mg protein in the crude lysates to below 50 EU/mg, as determined by the Pyrochrome Assay (Associates of Cape Cod, Inc., MA).

Native agarose gel electrophoresis (NAGE) and immunoblotting. NAGE was performed in 1% agarose gels (2.6% for T=3 vs. T=4 particle distinction; Supplementary Fig. S1a) as described⁸. For immunological detection, NAGE or SDS-PAGE gels were blotted to PVDF membranes which were probed with specific primary antibodies and peroxidase-conjugated secondary antibodies plus chemiluminescent substrates²⁹. Monoclonal anti-HBc antibodies used were 10E11 and 10F10 (anti-coreN and anti-coreC, respectively²⁷); 312 and 3105 (anti-c/e1^{13,58,59}); 275¹³ and 3120³⁵, both recognizing particle-specific epitopes.

Electron Microscopy. Negative staining EM using 2% uranyl acetate was performed as described³⁴.

Immunoglobulin binding by SC-SGFP-GB1 CLPs. For indirect immunofluorescence, 4% paraformaldehyde fixed HeLa cells were permeabilized using 0.2% Triton X-100 in PBS, blocked with 5% BSA in PBS and incubated with 0.05 µg/ml of mouse-anti-tubulin mAb, or not; for detection, either 0.13 µM goat-anti-mouse IgG antibody conjugated to Alexa488 (goxm-Alexa488; Invitrogen) or 0.05 µM SC-SGFP-GB1 CLPs were used. Images were taken with a Zeiss AxioVert 35 microscope. For fluorescent Western blot detection, a dilution series of recombinant GFP mixed with constant amounts (1 µg/lane) each of BSA and HBc149H6 was separated by SDS-PAGE and electroblotted to nitrocellulose membranes. After blocking, the blots were incubated with mouse-anti-GFP mAb (Roche), then with either 2.0 µg/ml goxm-Alexa488 or 2.5 µg/ml SC-SGFP-GB1 CLPs. Fluorescent signals were recorded using a Typhoon 7000 imager (GE Healthcare).

Details of the evaluation of the reactivity of SplitCore CLPs with human anti-HBc in commercial ELISAs and the immunizations with OspA- and CSP-presenting SplitCore CLPs are given in the Supplementary Protocols.

- Young, M., Willits, D., Uchida, M. & Douglas, T. Plant viruses as biotemplates for materials and their use in nanotechnology. *Annu Rev Phytopathol* **46**, 361–384 (2008).
- Manchester, M. & Steinmetz, N.F. Viruses and nanotechnology. Preface. *Curr Top Microbiol Immunol* **327**, v–vi (2009).
- Steinmetz, N.F. Viral nanoparticles as platforms for next-generation therapeutics and imaging devices. *Nanomedicine* **6**, 634–641 (2010).
- Plummer, E.M. & Manchester, M. Viral nanoparticles and virus-like particles: platforms for contemporary vaccine design. *Wiley Interdiscip Rev Nanomed Nanobiotechnol* doi: 10.1002/wnan.119 (2010).
- Whitacre, D.C., Lee, B.O. & Milich, D.R. Use of hepadnavirus core proteins as vaccine platforms. *Expert Rev Vaccines* **8**, 1565–1573 (2009).
- Crowther, R.A. *et al.* Three-dimensional structure of hepatitis B virus core particles determined by electron cryomicroscopy. *Cell* **77**, 943–950 (1994).
- Steven, A.C. *et al.* Structure, assembly, and antigenicity of hepatitis B virus capsid proteins. *Adv Virus Res* **64**, 125–164 (2005).
- Birnbaum, F. & Nassal, M. Hepatitis B virus nucleocapsid assembly: primary structure requirements in the core protein. *J Virol* **64**, 3319–3330 (1990).
- Watts, N.R. *et al.* The morphogenic linker peptide of HBV capsid protein forms a mobile array on the interior surface. *Embo J* **21**, 876–884 (2002).
- Böttcher, B., Wynne, S.A. & Crowther, R.A. Determination of the fold of the core protein of hepatitis B virus by electron cryomicroscopy. *Nature* **386**, 88–91 (1997).
- Conway, J.F. *et al.* Visualization of a 4-helix bundle in the hepatitis B virus capsid by cryo-electron microscopy. *Nature* **386**, 91–94 (1997).
- Wynne, S.A., Crowther, R.A. & Leslie, A.G. The crystal structure of the human hepatitis B virus capsid. *Mol Cell* **3**, 771–780 (1999).

- Salfeld, J., Pfaff, E., Noah, M. & Schaller, H. Antigenic determinants and functional domains in core antigen and e antigen from hepatitis B virus. *J Virol* **63**, 798–808 (1989).
- Fehr, T., Skrastina, D., Pumpens, P. & Zinkernagel, R.M. T cell-independent type I antibody response against B cell epitopes expressed repetitively on recombinant virus particles. *Proc Natl Acad Sci U S A* **95**, 9477–9481 (1998).
- Milich, D.R. & McLachlan, A. The nucleocapsid of hepatitis B virus is both a T-cell-independent and a T-cell-dependent antigen. *Science* **234**, 1398–1401 (1986).
- Pumpens, P. & Grens, E. HBV core particles as a carrier for B cell/T cell epitopes. *Intervirology* **44**, 98–114 (2001).
- Gregson, A.L. *et al.* Phase I trial of an alhydrogel adjuvanted hepatitis B core virus-like particle containing epitopes of Plasmodium falciparum circumsporozoite protein. *PLoS One* **3**, e1556 (2008).
- Taylor, K.M. *et al.* Influence of three-dimensional structure on the immunogenicity of a peptide expressed on the surface of a plant virus. *J Mol Recognit* **13**, 71–82 (2000).
- Nassal, M. *et al.* Development of hepatitis B virus capsids into a whole-chain protein antigen display platform: new particulate Lyme disease vaccines. *Int J Med Microbiol* **298**, 135–142 (2008).
- Ren, Z.J. *et al.* Phage display of intact domains at high copy number: a system based on SOC, the small outer capsid protein of bacteriophage T4. *Protein Sci* **5**, 1833–1843 (1996).
- Sternberg, N. & Hoess, R.H. Display of peptides and proteins on the surface of bacteriophage lambda. *Proc Natl Acad Sci U S A* **92**, 1609–1613 (1995).
- Kratz, P.A., Böttcher, B. & Nassal, M. Native display of complete foreign protein domains on the surface of hepatitis B virus capsids. *Proc Natl Acad Sci U S A* **96**, 1915–1920 (1999).
- Steere, A.C. & Glickstein, L. Elucidation of Lyme arthritis. *Nat Rev Immunol* **4**, 143–152 (2004).
- Skamel, C. *et al.* Hepatitis B virus capsid-like particles can display the complete, dimeric outer surface protein C and stimulate production of protective antibody responses against *Borrelia burgdorferi* infection. *J Biol Chem* **281**, 17474–17481 (2006).
- Ormö, M. *et al.* Crystal structure of the *Aequorea victoria* green fluorescent protein. *Science* **273**, 1392–1395 (1996).
- Kumaran, D. *et al.* Crystal structure of outer surface protein C (OspC) from the Lyme disease spirochete, *Borrelia burgdorferi*. *Embo J* **20**, 971–978 (2001).
- Li, H., Dunn, J.J., Luft, B.J. & Lawson, C.L. Crystal structure of Lyme disease antigen outer surface protein A complexed with an Fab. *Proc Natl Acad Sci U S A* **94**, 3584–3589 (1997).
- Nassal, M. *et al.* A fusion product of the complete *Borrelia burgdorferi* outer surface protein A (OspA) and the hepatitis B virus capsid protein is highly immunogenic and induces protective immunity similar to that seen with an effective lipidated OspA vaccine formula. *Eur J Immunol* **35**, 655–665 (2005).
- Walker, A., Skamel, C., Vorreiter, J. & Nassal, M. Internal core protein cleavage leaves the hepatitis B virus capsid intact and enhances its capacity for surface display of heterologous whole chain proteins. *J Biol Chem* **283**, 33508–33515 (2008).
- Kerppola, T.K. Bimolecular fluorescence complementation (BiFC) analysis as a probe of protein interactions in living cells. *Annu Rev Biophys* **37**, 465–487 (2008).
- Salis, H.M., Mirsky, E.A. & Voigt, C.A. Automated design of synthetic ribosome binding sites to control protein expression. *Nat Biotechnol* **27**, 946–950 (2009).
- Vogel, M., Vorreiter, J. & Nassal, M. Quaternary structure is critical for protein display on capsid-like particles (CLPs): efficient generation of hepatitis B virus CLPs presenting monomeric but not dimeric and tetrameric fluorescent proteins. *Proteins* **58**, 478–488 (2005).
- Porterfield, J.Z. *et al.* Full-length hepatitis B virus core protein packages viral and heterologous RNA with similarly high levels of cooperativity. *J Virol* **84**, 7174–7184 (2010).
- Böttcher, B., Vogel, M., Ploss, M. & Nassal, M. High plasticity of the hepatitis B virus capsid revealed by conformational stress. *J Mol Biol* **356**, 812–822 (2006).
- Conway, J.F. *et al.* Characterization of a conformational epitope on hepatitis B virus core antigen and quasidequivalent variations in antibody binding. *J Virol* **77**, 6466–6473 (2003).
- Liu, S. *et al.* Removal of endotoxin from recombinant protein preparations. *Clin Biochem* **30**, 455–463 (1997).
- Zhong, W. *et al.* Therapeutic passive vaccination against chronic Lyme disease in mice. *Proc Natl Acad Sci U S A* **94**, 12533–12538 (1997).
- Ding, W. *et al.* Structural identification of a key protective B-cell epitope in Lyme disease antigen OspA. *J Mol Biol* **302**, 1153–1164 (2000).
- Casares, S., Brumeau, T.D. & Richie, T.L. The RTS,S malaria vaccine. *Vaccine* **28**, 4880–4894 (2010).
- Milich, D.R., McLachlan, A., Thornton, G.B. & Hughes, J.L. Antibody production to the nucleocapsid and envelope of the hepatitis B virus primed by a single synthetic T cell site. *Nature* **329**, 547–549 (1987).
- Plassmeyer, M.L. *et al.* Structure of the Plasmodium falciparum circumsporozoite protein, a leading malaria vaccine candidate. *J Biol Chem* **284**, 26951–26963 (2009).
- Cerami, C. *et al.* The basolateral domain of the hepatocyte plasma membrane bears receptors for the circumsporozoite protein of Plasmodium falciparum sporozoites. *Cell* **70**, 1021–1033 (1992).



43. Billaud, J.N. *et al.* Advantages to the use of rodent hepadnavirus core proteins as vaccine platforms. *Vaccine* **25**, 1593–1606 (2007).
44. Cabantous, S., Terwilliger, T.C. & Waldo, G.S. Protein tagging and detection with engineered self-assembling fragments of green fluorescent protein. *Nat Biotechnol* **23**, 102–107 (2005).
45. Stiles, B.G., Garza, A.R., Ulrich, R.G. & Boles, J.W. Mucosal vaccination with recombinantly attenuated staphylococcal enterotoxin B and protection in a murine model. *Infect Immun* **69**, 2031–2036 (2001).
46. Jegerlehner, A. *et al.* Carrier induced epitopic suppression of antibody responses induced by virus-like particles is a dynamic phenomenon caused by carrier-specific antibodies. *Vaccine* **28**, 5503–5512 (2010).
47. De Filette, M. *et al.* Universal influenza A M2e-H3c vaccine protects against disease even in the presence of pre-existing anti-H3c antibodies. *Vaccine* **26**, 6503–6507 (2008).
48. Geldmacher, A. *et al.* A hantavirus nucleocapsid protein segment exposed on hepatitis B virus core particles is highly immunogenic in mice when applied without adjuvants or in the presence of pre-existing anti-core antibodies. *Vaccine* **23**, 3973–3983 (2005).
49. Michnick, S.W., Ear, P.H., Manderson, E.N., Remy, I. & Stefan, E. Universal strategies in research and drug discovery based on protein-fragment complementation assays. *Nat Rev Drug Discov* **6**, 569–582 (2007).
50. Lee, B.O. *et al.* Interaction of the hepatitis B core antigen and the innate immune system. *J Immunol* **182**, 6670–6681 (2009).
51. Beterams, G., Böttcher, B. & Nassal, M. Packaging of up to 240 subunits of a 17 kDa nuclease into the interior of recombinant hepatitis B virus capsids. *FEBS Lett* **481**, 169–176 (2000).
52. Popp, M.W., Antos, J.M., Grotenbreg, G.M., Spooner, E. & Ploegh, H.L. Sortagging: a versatile method for protein labeling. *Nat Chem Biol* **3**, 707–708 (2007).
53. Finn, M.G. & Fokin, V.V. Click chemistry: function follows form. *Chem Soc Rev* **39**, 1231–1232 (2010).
54. Strable, E. *et al.* Unnatural amino acid incorporation into virus-like particles. *Bioconjug Chem* **19**, 866–875 (2008).
55. Manayani, D.J. *et al.* A viral nanoparticle with dual function as an anthrax antitoxin and vaccine. *PLoS Pathog* **3**, 1422–1431 (2007).
56. Nassal, M. Total chemical synthesis of a gene for hepatitis B virus core protein and its functional characterization. *Gene* **66**, 279–294 (1988).
57. Bichko, V. *et al.* Epitopes recognized by antibodies to denatured core protein of hepatitis B virus. *Mol Immunol* **30**, 221–231 (1993).
58. Belnap, D.M. *et al.* Diversity of core antigen epitopes of hepatitis B virus. *Proc Natl Acad Sci U S A* **100**, 10884–10889 (2003).
59. Conway, J.F. *et al.* Hepatitis B virus capsid: localization of the putative immunodominant loop (residues 78 to 83) on the capsid surface, and implications for the distinction between c and e-antigens. *J Mol Biol* **279**, 1111–1121 (1998).

Acknowledgements

This work was supported in part by the Deutsche Forschungsgemeinschaft (DFG). We thank Jolanta Vorreiter for excellent technical assistance. We are indebted to many colleagues for their contributions to specific aspects: Bettina Böttcher (University of Edinburgh, U.K.), Britta Gerlach and Simone Prinz (EMBL, Heidelberg, Germany) for electron microscopy; Thomas Stehle and Markus M. Simon (Max-Planck-Institute for Immunobiology, Freiburg, Germany) for characterizing immunogenicity and protective potential of SplitCore-OspA CLPs; and Jean-Noel Billaud and David Milich (Vaccine Research Institute of San Diego) for the SplitCore-CSP immunizations.

Author contributions

CS performed and designed experiments and analyzed data. JW performed and designed experiments, analyzed data and assisted in writing and editing the manuscript. MN designed and performed the initial experiments, designed, analyzed and interpreted others and wrote the manuscript.

Additional information

Supplementary Information accompanies this paper at <http://www.nature.com/scientificreports>

Competing financial interests: The authors declare competing financial interests. Authors MN and CS are, and author AW has been, employed by the Universitätsklinikum Freiburg which has filed a patent application for the SplitCore system described in this report [Ref: WO/2008/028535] with the authors listed as inventors.

License: This work is licensed under a Creative Commons Attribution-NonCommercial-NoDerivative Works 3.0 Unported License. To view a copy of this license, visit <http://creativecommons.org/licenses/by-nc-nd/3.0/>

How to cite this article: Walker, A., Skamel, C. & Nassal M. SplitCore: An exceptionally versatile viral nanoparticle for native whole protein display regardless of 3D structure. *Sci. Rep.* **1**, 5; DOI: 10.1038/srep00005 (2011).